environmental microbiology

Environmental Microbiology (2022) **24**(4), 2078–2088 doi:10.1111/1462-2920.15960

CotG controls spore surface formation in response to the temperature of growth in *Bacillus subtilis*

Giovanni Di Gregorio Barletta,[‡] Maria Vittoria,[‡] Mariamichela Lanzilli,[†] Claudia Petrillo, Ezio Ricca[*] and Rachele Isticato

Department of Biology, Federico II University, Naples, Italy.

Summary

Bacterial spores of the *Bacillus* genus are ubiquitous in nature and are commonly isolated from a variety of diverse environments. Such wide distribution mainly reflects the spore resistance properties but some *Bacillus* species can grow/sporulate in at least some of the environments where they have been originally isolated. Growing and sporulating at different conditions is known to affect the structure and the resistance properties of the produced spore. In *B. subtilis* the temperature of growth and sporulation has been shown to influence the structure of the spore surface throughout the action of a sporulation-specific and heat-labile kinase CotH. Here we report that CotG, an abundant component of the *B. subtilis* spore surface and a substrate of the CotH kinase, assembles around the forming spore but also accumulates in the mother cell cytoplasm where it forms aggregates with at least two other coat components. Our data suggest that the thermo-regulator CotH contributes to the switch between the coat of 25°C and that of 42°C spores by controlling the phosphorylation levels of CotG that, in turn, regulates the assembly of at least two other coat components.

Introduction

Spore formers are mostly Gram-positive bacteria of the *Bacillus* and *Clostridiales* genera sharing the ability to differentiate into a quiescent and resistant cell, the spore, in response to environmental conditions no longer allowing cell growth. The spore can survive almost indefinitely without water and nutrients and at conditions of extreme temperature and pH, and in the presence of toxic chemicals and lytic enzymes (McKenney *et al*., 2013). Although quiescent, the spore senses the environment and responds to the presence of nutrients by germinating and forming a new cell able to grow and eventually sporulate (Christie and Setlow, 2020). Spore resistance is in part due to the spore structure, characterized by a dehydrated cytoplasm surrounded by protective layers: a peptidoglycan-like cortex and a proteinaceous and multilayered coat (McKenney *et al*., 2013). In some species, such as *Bacillus anthracis* or *Clostridioides difficile*, the outer coat is surrounded by the exosporium, an additional layer formed by proteins and glycoproteins (McKenney *et al*., 2013). In *B. subtilis*, the model system for spore formers, the coat is surrounded by the crust, an additional layer formed by proteins and glycoproteins, in some respect resembling the exosporium of other species (McKenney *et al*., 2013).

Spores are ubiquitous in nature and are commonly isolated from almost all environments where they have been searched for, from desert sands and deep sediments, to the gut of animals and insects (Isticato *et al*., 2020). In some of these diverse environments, such as the animal gut (Cutting, 2011), the rhizosphere of plants (Timmusk *et al*., 2011) and the deep marine sediments (Cupit *et al*., 2019), spores of some *Bacillus* species germinate, proliferate and sporulate, indicating a physiological role of aerobic spore formers in those specific environments. The conditions of growth and sporulation influence the structure of the spore (Garcia *et al*., 2010; Abhyankar *et al*., 2016) and recent reports have shown that the temperature of sporulation modifies the structure of the spore coat and of the exosporium in *B. cereus* (Bressuire-Isoard *et al*., 2016) and induces a switch between two alternative types of spore surfaces in *B. subtilis* (Isticato *et al*., 2020). The latter study identified CotH, an atypical Ser/Tyr kinase, as a major thermo-regulator of the spore surface, more abundant and active at low (25°C) than at high (42°C) temperatures and able to induce a switch from the 25°C to the 42°C spore surface (Isticato *et al*., 2020).

In *B. subtilis* the gene coding for the kinase CotH is clustered with the genes coding for two coat proteins that

Received 27 December, 2021; accepted 25 February, 2022. *For correspondence. E-mail ericca@unina.it; Tel. (+39)081679036; Fax (+39)081679233. [‡]These two authors contributed equally. [†]Present address: Institute of Biomolecular Chemistry, National Research Council of Italy, Pozzuoli, Naples, Italy.

are the only two CotH substrates, CotB and CotG (Nguyen *et al*., 2016; Freitas *et al*., 2020). While the *cotB* gene follows the 3′ end of *cotH* and is independently transcribed (Donovan *et al*., 1987), the *cotG* gene is at the 5′ end of *cotH* but divergently transcribed and entirely contained between the promoter and the coding region of *cotH* (Giglio *et al*., 2011). Both *cotG* and *cotH* genes are transcribed by SigK-controlled RNA polymerase but are differently regulated by the transcription factor GerE, which acts as an activator of *cotG* (Sacco *et al*., 1995) and a repressor of *cotH* (Naclerio *et al*., 1996). Although *cotG* mRNA is complementary to the 5′ un-translated part of the *cotH* mRNA, it does not have a role in *cotH* expression (Giglio *et al*., 2011).

CotG is an abundant coat protein of 195 amino acids with a strong positive charge (Sacco *et al*., 1995) and is listed in the top-20 supercharged proteins present in data banks (Ma *et al*., 2020). Such positive charge is, at least partially, balanced by its extensive and CotH-dependent phosphorylation (Saggese *et al*., 2014; Nguyen *et al*., 2016; Freitas *et al*., 2020). In a *B. subtilis* mutant lacking CotH, unphosphorylated CotG affects the coat assembly of other proteins, such as CotC and CotU (Saggese *et al*., 2014).

It has been previously reported that *cotG* is transcribed about twofold more efficiently in cells sporulating at 25°C or 37°C than at 42°C, while *cotC*, *cotU* and *cotH* have similar transcription levels at the three temperatures (Nicolas *et al*., 2012). In addition, the temperature also controls the stability of the kinase CotH, which is more stable at low than high temperatures (Isticato *et al*., 2020). As a consequence, at a low temperature (25°C), when the kinase CotH is abundantly present and active, its substrates CotB and CotG are efficiently phosphorylated and assembled on the coat surface contributing to the lamellar-like and electron-dense appearance of 25°C spores (Isticato *et al*., 2020). At a high temperature (42°C) CotH is less active (or totally inactive), CotB and CotG are less efficiently phosphorylated and assembled on the coat where are replaced by other proteins, including CotC and CotU, which contribute to the granular and thick appearance of the coat of 42°C spores (Isticato *et al*., 2020). The focus of this study is CotG and its negative effect on the assembly of CotC and CotU. We report that such negative effect is due to the unphosphorylated form of CotG that accumulates in the mother cell cytoplasm and forms aggregates with CotC and CotU. It is proposed that the negative effect observed in a mutant lacking CotH is the exacerbation of a regulatory role of CotG, that in a wild type cell controls the amounts of CotC and CotU assembled around the forming spore in response to the temperature of growth and sporulation.

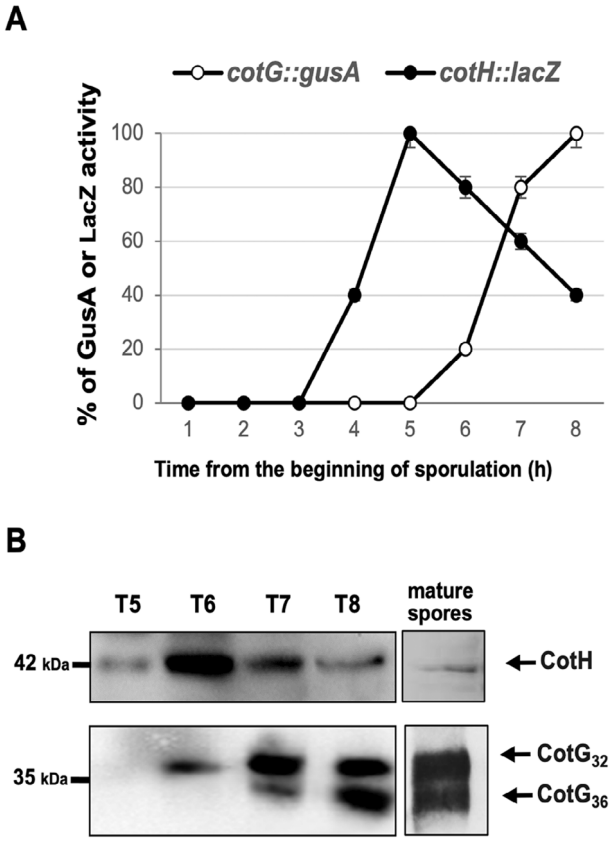

Fig. 1. Timing of production of CotG and CotH during sporulation.
A. Temporal expression of the *cotH* (closed symbols) and *cotG* (open symbols) genes in *B. subtilis* strain GC224, carrying the *cotG*::*gusA* and *cotH*::*lacZ* fusions.
B. Detection of CotH and CotG proteins by Western blotting analysis of proteins extracted from wild-type sporulating cells and mature spores reacted against anti-CotH or anti-CotG primary antibodies. Peroxidase-conjugated anti-rabbit secondary antibodies were used to visualize the recognized proteins.

Result and discussion

CotG accumulates in the mother cell cytoplasm

The *cotG* and *cotH* genes are both controlled by the sporulation-specific sigma factor of the RNA polymerase SigK in conjunction with the transcriptional factor GerE that activates *cotG* (Sacco *et al*., 1995) and represses *cotH* (Naclerio *et al*., 1996), presumably regulating the timing of *cotG* and *cotH* expression during sporulation. We monitored the expression of both genes simultaneously in sporulating cells of a strain carrying the *cotH* and *cotG* genes translationally fused to the *lacZ* and *gusA* genes of *E. coli* respectively. As expected, the *cotH*::*lacZ* fusion was expressed earlier than the *cotG*::*gusA* and its highest levels of expression were observed 5 h after the beginning of sporulation (T5) when *cotG* expression had not yet started (Fig. 1A). At late sporulation times, *cotH* expression

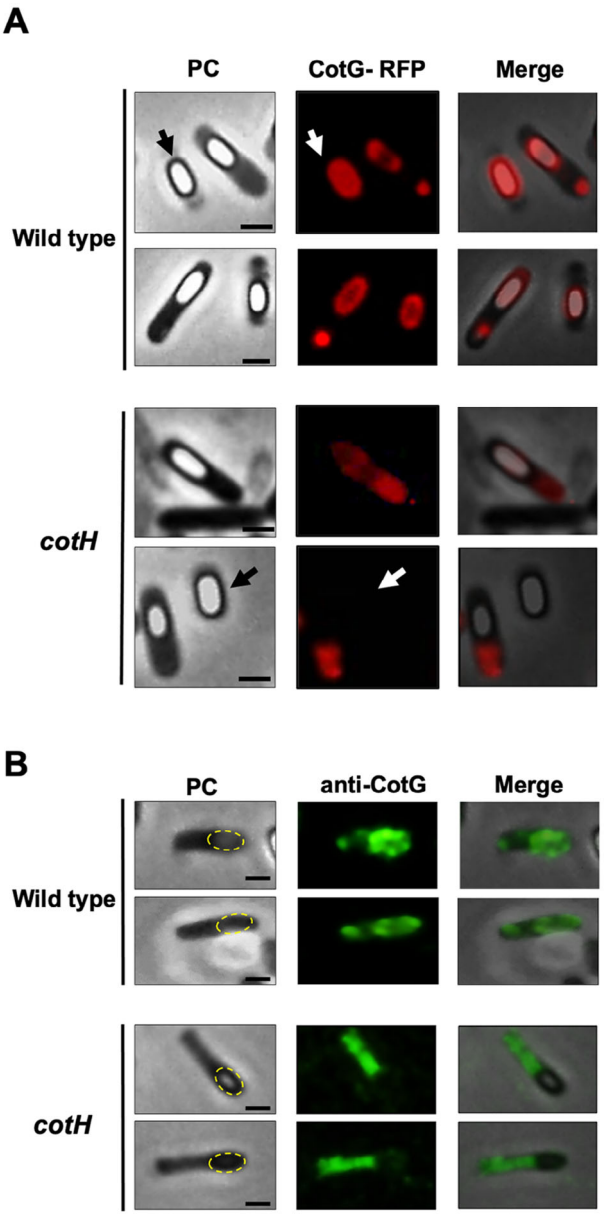

Fig. 2. Fluorescence microscopy detection of CotG.
A. Fluorescence of the CotG-RFP fusion was analysed in an otherwise wild type (RH296) and isogenic mutant lacking *cotH* (RH298). Arrows indicate mature spores observed by phase-contrast (black arrows) and fluorescence (white arrows) microscopy.
B. Immunofluorescence analysis of wild type (PY79) and isogenic *cotH* (ER220) mutant sporangia with anti-CotG antibody. For both panels, the percentage of cells showing the indicated fluorescence is reported in Supplementary Material Table S3. Representative microscopy fields are reported for each experiment and strain. PC: phase contrast. The exposure time was 500 ms in all cases. Scale bar 1 μm.

rapidly declined while *cotG* expression increased (Fig. 1A). Consistently, in a wild type strain [PY79 (Youngman *et al*., 1984)] the kinase CotH was detected in extracts from sporulating cells 5 h after the beginning of sporulation (T5), reached its maximal abundance 1 h later (T6) and then rapidly decreased while CotG appeared at T6 and became abundant at later times (Fig. 1B). As previously reported (Freitas *et al*., 2020), CotG was extracted from prespores and mature spores in two forms, a slower migrating form of about 36 kDa ($CotG_{36}$) and a faster migrating form of about 32 kDa ($CotG_{32}$) (Fig. 1B). $CotG_{36}$ appeared first at T6, and $CotG_{32}$ 1 h later, although was less abundant than $CotG_{36}$ (Fig. 1B). Then, at T8 and in mature spores the two CotG forms were similarly represented (Fig. 1B).

The observation that CotG is produced and accumulates at late time of sporulation, when the amount of the specific kinase CotH is decreasing (Fig. 1), raised the possibility that some CotG molecules could be present in sporangia in an unphosphorylated form. Repeated attempts to detect CotG by Western blotting in the mother cell cytoplasm were unsuccessful, therefore a fluorescence microscopy approach was followed using strain RH296 of *B. subtilis* carrying the *cotG* gene fused to the gene coding for the red fluorescent protein (RFP) of the coral *Discosoma* sp. (Donadio *et al*., 2016; Isticato *et al*., 2020). In an otherwise wild type strain most CotG-RFP molecules were localized around the forming spore (Fig. 2A); however, some CotG-RFP molecules were also observed in the mother cells, concentrated in well-defined small spots (Fig. 2A). In an isogenic strain lacking the kinase CotH (RH298), CotG is not phosphorylated and not assembled around the forming spore (Freitas *et al*., 2020); as a consequence a strong fluorescence signal (CotG-RFP) almost completely filled the mother cell cytoplasm (Fig. 2A). The dependency of CotG-RFP accumulation in the mother cell cytoplasm on CotH (Fig. 2A) makes it unlikely that the fluorescence observed in the mother cell of a wild type strain (Fig. 2A) was due to RFP alone (i.e. due to RFP cleaved off from CotG). However, to confirm this point, an immunofluorescence microscopy analysis was performed with anti-CotG antibody. As shown in Fig. 2B, CotG-specific fluorescence signals were observed around the forming spore and in the mother cell cytoplasm of a wild type strain, where they formed well-defined spots similar to those observed with CotG-RFP (Fig. 2A). In a mutant lacking CotH all CotG-dependent fluorescence was found in the mother cell cytoplasm (Fig. 2B).

Results of Figs 1 and 2 indicate that in a wild type strain some CotG molecules do not assemble around the spore and accumulate in the mother cell cytoplasm in well-defined spots. In a mutant lacking CotH such accumulation is massive and obviously formed by unphosphorylated CotG.

CotG is mostly unphosphorylated in the mother cell cytoplasm of wild type sporangia

To verify whether the CotG molecules present in the mother cell of a wild type strain were phosphorylated,

immunofluorescence experiments were performed with anti-PKC antibody (Cell Signalling Technology), recognizing phosphorylated serine residues surrounded by a lysine or an arginine. In a wild type strain (PY79) a strong fluorescence signal was observed associated to the forming spore while only a modest and diffuse signal was visible in the mother cell cytoplasm (Fig. 3). No fluorescence was observed in a mutant lacking CotH (AZ607), indicating that the fluorescence in wild type sporangia was only due to the kinase activity of CotH (Fig. 3). In a mutant lacking CotB (AZ668), the other substrate of the kinase CotH, fluorescence signals were only due to the CotH-dependent phosphorylation of CotG and appeared mainly present around the forming spore (Fig. 3). In sporangia of strain AZ668 only a minimal part of the fluorescence (due to phosphorylated CotG molecules) was found in the cytoplasm, never forming the well-defined fluorescence spot observed in Fig. 2.

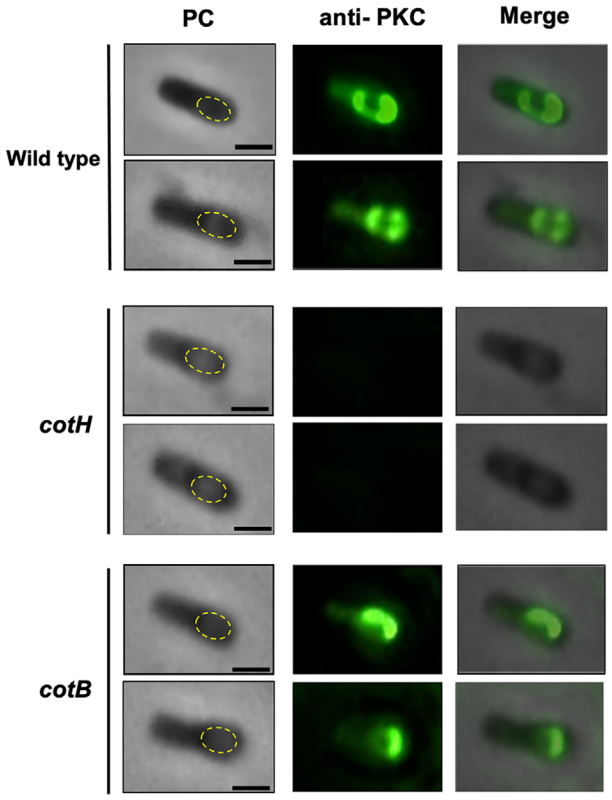

Fig. 3. Fluorescence microscopy detection of phosphorylated CotG. Immunofluorescence analysis of sporangia of wild type (PY79) and isogenic mutants lacking *cotH* (AZ607) and *cotB* (AZ668) with anti-PKC antibody. For all panels, the percentage of cells showing the indicated fluorescence is reported in Supplementary Material Table S3. Representative examples are reported by phase-contrast (PC) and fluorescence microscopy and by merging the images (Merge). In PC panels dotted yellow ovals indicate the position of the forming spore. The exposure time was 200 ms in all cases. Scale bar 1 μm.

Based on these results, we infer that in a wild type strain most CotG molecules are phosphorylated and assembled around the spore, the remaining CotG molecules are mostly unphosphorylated and form well-defined spots in the mother cell cytoplasm.

Unphosphorylated CotG forms aggregates with CotC and CotU

Accumulation of massive amounts of unphosphorylated, supercharged CotG in the mother cell cytoplasm of a mutant strain lacking CotH (Fig. 2A) could be the cause of the mis-assemblage of the coat proteins CotC and CotU previously observed in mature spores of a *cotH* mutant strain (Saggese *et al*., 2014). To verify such hypothesis, immunofluorescence microscopy experiments were performed with anti-CotC antibody, known to recognize both CotC and CotU proteins (Isticato *et al*., 2004; Isticato *et al*., 2008). In a wild type strain (PY79), fluorescence signals were mostly observed around the forming spore and only a weak fluorescence was localized in the mother cell (Fig. 4). Fluorescence signals similar to those observed in wild type sporangia but of reduced intensity were also observed in mutants lacking CotC (RH101) or CotU (RH202) (Fig. 4), indicating that the fluorescence observed in wild type sporangia was due to both CotC and CotU.

In a mutant lacking CotH (AZ607) the CotC/CotU-dependent fluorescence signals appeared was differently distributed between the forming spore and mother cell with respect to the wild type strain, with a stronger signal in the mother cell cytoplasm and weaker signal around the spore than in the isogenic wild type strain (Fig. 4). The weak assemblage of CotC/CotU around the forming spore is however transient, since no CotC/CotU are then observed around mature spores of a mutant lacking CotH (Saggese *et al*., 2014). Therefore, in a mutant lacking CotH both unphosphorylated CotG (Fig. 2) and CotC/CotU (Fig. 4) accumulated in the mother cell cytoplasm in well-defined spots. Such effect is CotG-dependent since it was not observed in a mutant lacking CotG (AZ604) (Fig. 4).

A fluorescence microscopy analysis of the *B. subtilis* strain RH406, carrying the RFP fused to CotG and the green fluorescent protein (GFP) fused to CotC (Isticato *et al*., 2020) confirmed that both CotC and CotG behave similarly and showed that the two proteins co-localize in the mother cell cytoplasm (Fig. 5). In an otherwise wild type strain both CotG-RFP and CotC-GFP were mostly localized around the forming spores but were also present in the mother cell cytoplasm (Fig. 5). When CotH was not present, only few CotG-RFP and CotC-GPF molecules were around the forming spore while most of them failed to assemble around the spore and were co-localized in aggregates in the mother cell cytoplasm (Fig. 5).

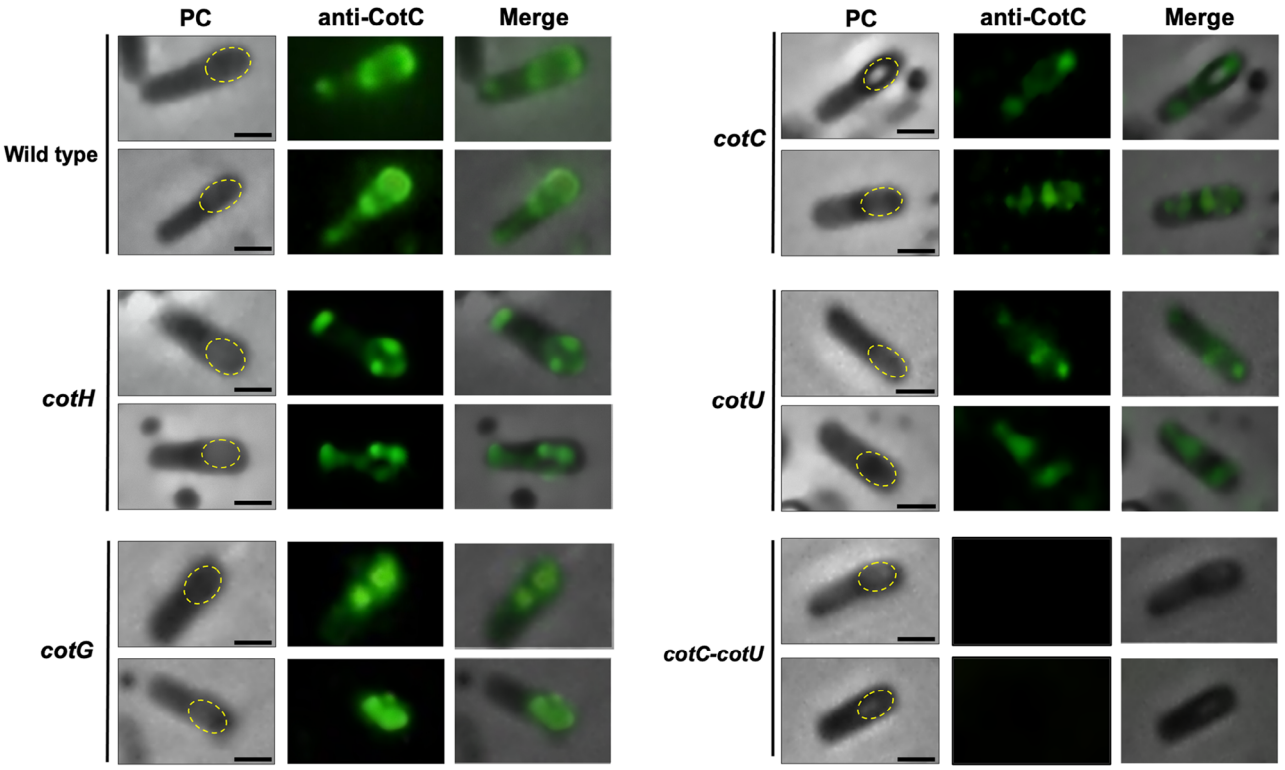

Fig. 4. Fluorescence microscopy detection of CotC and CotU. Immunofluorescence analysis of sporangia of wild type and isogenic mutants lacking *cotH* (AZ607), *cotG* (AZ604), *cotC* (RH101), or *cotU* (RH202) with anti-CotC antibody. For all panels, the percentage of cells showing the indicated fluorescence is reported in Supplementary Material Table S3. Representative examples are reported by phase-contrast (PC) and fluorescence (anti-CotC) microscopy and by merging the images (Merge). In PC panels dotted yellow ovals indicate the position of the forming spore. The exposure time was 1000 ms in all cases. Scale bar 1 μm.

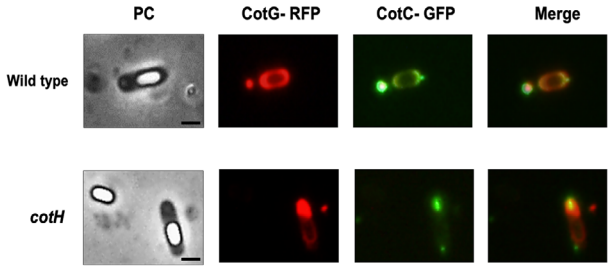

Fig. 5. Fluorescence microscopy detection of CotG-RFP and CotC-GFP. The two gene fusions, *cotG*::*rfp* and *cotC*::*gfp*, were analysed in an otherwise wild type (PY79) and in an isogenic mutant lacking *cotH* (AZ607). For all panels, the percentage of cells showing the indicated fluorescence is reported in Supplementary Material Table S3. Representative examples are reported for each experiment and strain. The exposure time was 500 ms for both fusions. Scale bar 1 μm.

The behaviour observed with CotC/CotU was not observed with other coat proteins, independently from their dependence on CotG in a mutant lacking CotH (Saggese *et al*., 2014). Indeed, CotS (affected by CotG), CotA and CotZ (not affected by CotG) (Saggese *et al*., 2014) were all found assembled around the forming spore with no fluorescence signals in the mother cell cytoplasm, both in a wild type and in a strain bearing a *cotH* null mutation (Fig. 6). Results of Fig. 6 then suggest that the formation of CotG-dependent aggregates is not common to all coat proteins but rather a specific property of CotC and CotU.

CotG controls the assembly of CotC and CotU in wild type sporangia in response to the temperature

A fluorescence microscopy analysis of *B*. *subtilis* strains carrying the *cotC*::*gfp* or the *cotG*::*rfp* fusion was performed on sporangia grown at 25°C and 42°C. Since the temperature affects the growth rate, the entry into the sporulation cycle and the time of spore formation, sporangia of similar age were produced at the different temperatures as previously described (Isticato *et al*., 2020). As shown in Fig. 7A, CotC and CotG molecules showed an opposite behaviour in sporangia grown at 25°C or 42°C. At 25°C CotG-RFP was abundant around the spore and formed well-defined spots in the cytoplasm while CotC-GFP was almost absent around the spore and localized in well-defined spots in the cytoplasm (Fig. 7A). At 42°C CotG-RFP was almost absent

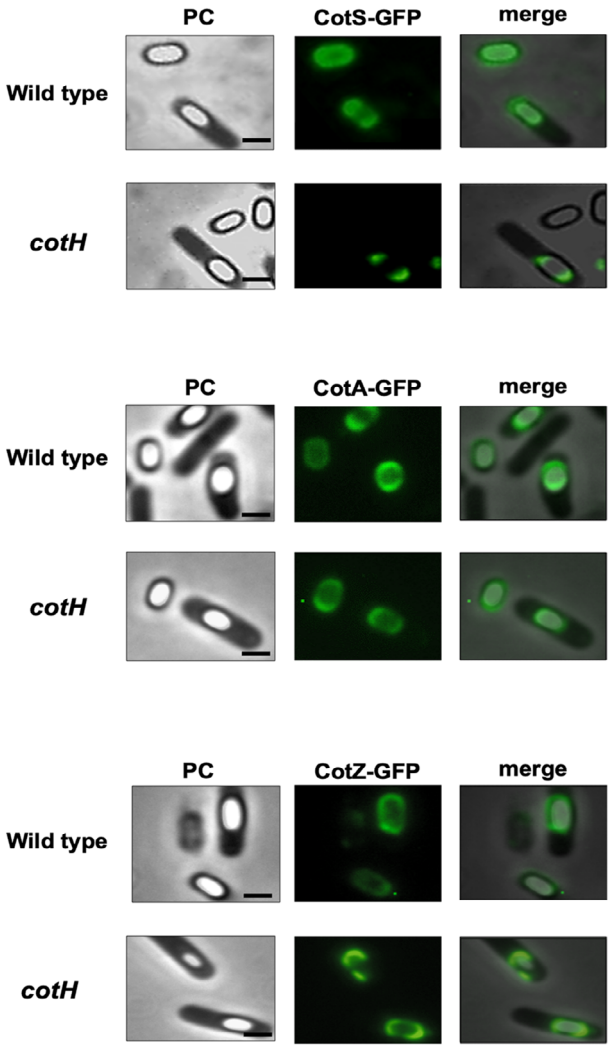

Fig. 6. Fluorescence microscopy detection of CotS, CotA and CotZ. *cotS*::*gfp*, *cotA*::*gfp* and *cotZ*::*gfp* fusions in an otherwise wild type strain (AZ644, AZ565 and AZ573 respectively) and in an isogenic mutant lacking *cotH* (AZ647, RH240 and RH278 respectively) analysed by fluorescence microscopy. The percentage of cells showing the indicated fluorescence is reported in Supplementary Material Table S3. Representative examples are reported for each experiment and strain. The exposure time was 500 ms in all cases. Scale bar 1 μm.

around the spore and formed well-defined spots in the cytoplasm while CotC-GFP was abundant around the spore and in minimal amounts in the cytoplasm (Fig. 7A). At 42°C CotG-RFP appeared less abundant than at 25°C, suggesting a reduced production of the protein. To clarify this point an isogenic strain carrying a translational *cotG*::*lacZ* fusion (Sacco *et al*., 1995) was grown at 25°C, 37°C and 42°C. As shown in Fig. 7B, the expression of the *cotG* genes was highest at 25°C, about twofold lower at 37°C and about threefold lower at 42°C, in agreement with a previous transcriptomic study (Nicolas *et al*., 2012).

To evaluate the phosphorylation status of CotG at different temperatures, an immunofluorescence analysis with anti-PKC on sporangia growing at 25°C and 42°C was performed. At low temperature CotG around the spore appeared mostly phosphorylated while in the mother cell cytoplasm was mostly unphosphorylated (Fig. 7C), similarly to what was observed at 37°C (Fig. 3). As expected by the low activity of the kinase CotH at 42°C (Isticato *et al*., 2020), at high temperature only a minimal amount of CotG was phosphorylated and exclusively found around the forming spore (Fig. 7C).

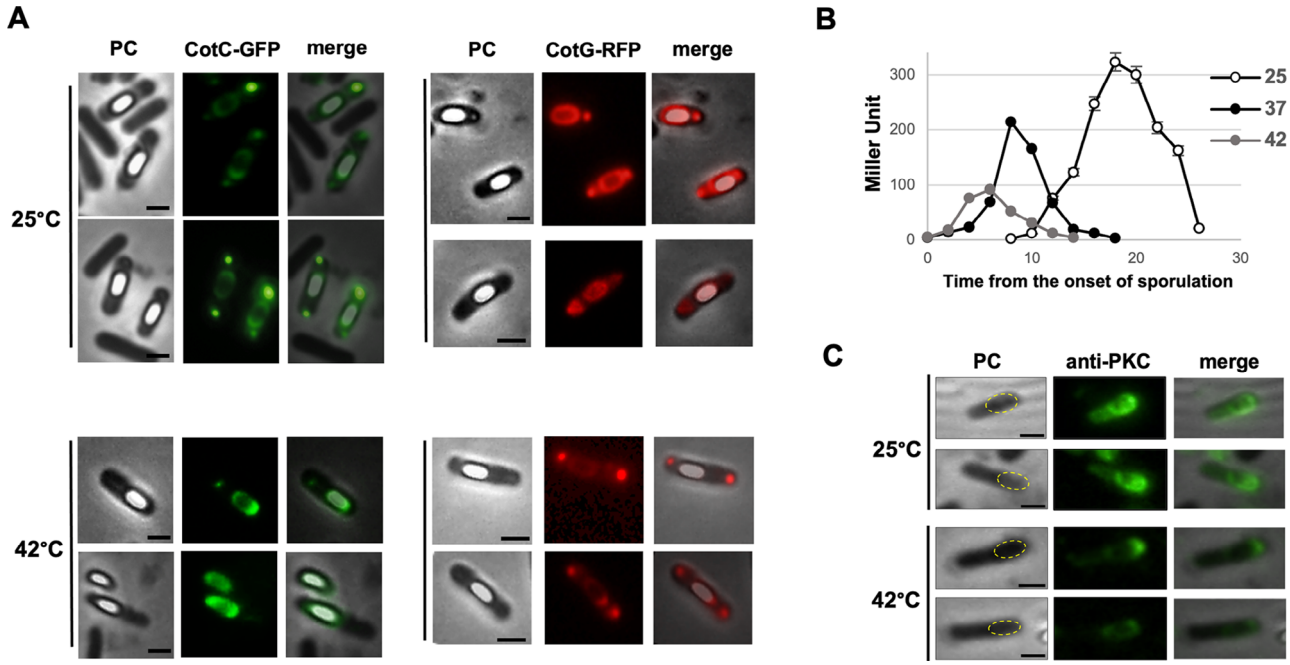

Fig. 7. Effect of the sporulation temperature on CotG and CotC assembly.
A. Fluorescence microscopy analysis of strains carrying the *cotC*::*gfp* (RH238) or *cotG*::*rfp* (RH296) fusion in sporulating cells produced at 25°C or 42°C. The percentage of cells showing the indicated fluorescence is reported in Supplementary Material Table S3. Representative examples are reported for each experiment and strain. The exposure time was 500 ms in all cases. Scale bar 1 μm.
B. *cotG*-directed β-galactosidase synthesis during sporulation at 25°C, 37°C and 42°C. Due to the reduced growth rate at 25°C, cells were collected at late times according to Isticato *et al*. (2020).
C. Immunofluorescence analysis of wild type (PY79) sporangia growing at 25°C or 42°C with anti-PKC antibody. The percentage of cells showing the indicated fluorescence is reported in Supplementary Material Table S3. Representative examples are reported by phase-contrast (PC) and fluorescence microscopy and by merging the images (Merge). In PC panels dotted yellow ovals indicate the position of the forming spore. The exposure time was 200 ms in all cases. Scale bar 1 μm.

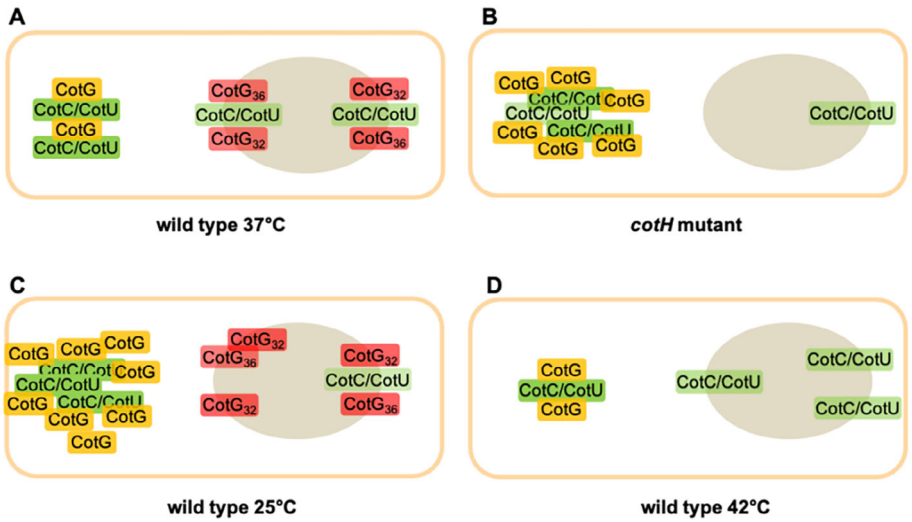

Fig. 8. Working model of CotG, CotC and CotU assembly at 37°C (A), in a mutant lacking CotH (B) and in a wild type strain at 25°C (C) or 42°C (D). Phosphorylated and unphosphorylated CotG molecules are boxed in red and yellow respectively.

Altogether, results of Fig. 7 suggest that at 25°C unphosphorylated CotG molecules accumulate in the cytoplasm sequestering most CotC (and presumably CotU) molecules in well-defined cytoplasmic spots and thus impairing their assembly around the spore. At 42°C less CotG molecules are produced, a minimal amount is phosphorylated and assembled around the spore while the remaining part is unphosphorylated and forms

aggregates with CotC (and presumably CotU), slightly reducing their assembly around the spore.

A model to explain the assembly of CotG and its regulatory role on the assembly of CotC/CotU is proposed in Fig. 8. In a wild type strain growing at 37°C, CotG is readily phosphorylated by CotH originating $CotG_{36}$ and $CotG_{32}$ (boxed in red in Fig. 8A). Some CotG molecules produced later in sporulation, when the kinase is no longer synthesized, are not phosphorylated and accumulate in the mother cell cytoplasm (boxed in yellow in Fig. 8A), where they form aggregates with CotC/CotU. As a result, both CotG and CotC/CotU are found around the spore and in the cytoplasm with CotG localization depending on its phosphorylation level (and therefore on CotH) and CotC/CotU localization depending on the level of unphosphorylated CotG (Fig. 8A). Under unphysiological conditions (in a mutant lacking CotH), all CotG molecules are unphosphorylated, massively accumulate in the cytoplasm sequestering all CotC/CotU molecules (Fig. 8B), and causing the previously reported negative effect of CotG on CotC/CotU assembly (Saggese *et al*., 2014). At 25°C CotG is abundant both around the spore and in the cytoplasm, where it sequesters a large part of the CotC/CotU molecules limiting their assemblage around the spore (Fig. 8C). At 42°C less CotG is produced but being almost completely unphosphorylated, does not assemble and accumulates in the cytoplasm sequestering some CotC/CotU molecules and thus regulating their assembly around the spore (Fig. 8D).

Conclusions

The main results in this manuscript are that *B*. *subtilis* controls by CotH-mediated phosphorylation the assembly of CotG and that unphosphorylated CotG accumulates in the mother cell cytoplasm forming aggregates with CotC and CotU. These results provide a possible mechanism to explain how *B*. *subtilis* builds different spores at different temperatures with those produced at 25°C being lamellar and heavily electron dense and those produced at 42°C appearing granular and thick (Isticato *et al*., 2020).

It has been previously proposed that CotH, a thermolabile kinase, phosphorylates CotG and CotB that are then readily assembled on the forming spores and contribute to the structure/function of the 25°C spore (Isticato *et al*., 2020). At 42°C CotH is almost totally absent/inactive, its phosphorylation targets, CotG and CotB, are almost undetectable on the spore surface where are replaced by other coat components, including CotC and CotU (Isticato *et al*., 2020). Results reported here suggest that unphosphorylated CotG forms aggregates with CotC and CotU, sequesters them in the mother cell cytoplasm and renders them unavailable for coat assemblage. Since the level of phosphorylated/assembled or unphosphorylated/unassembled CotG depends on the action of the thermo-sensor CotH, a hierarchical model is proposed to explain the effects of the temperature on the formation of the spore surface, with the temperature acting on *cotG* transcription (by still unexplored mechanism) and on the thermo-labile kinase CotH that controls its substrate CotG that, in turn, controls the assembly of CotC/CotU.

The unphosphorylated CotG accumulated in the cytoplasm has a strong positive charge [Net Charge Density (NCD) = 0.30 as defined by Ma *et al*., 2020] that may be responsible for the formation of the cytoplasmic aggregates. This hypothesis is supported by the previous observation that a mutant form of CotG, deleted of the central region where most of the positively charged amino acids are concentrated, and showing an NCD = 0.15, does not have any negative effect on the assembly of CotC/CotU (Saggese *et al*., 2016).

CotG of *B*. *subtilis* is not highly conserved but a CotG-like protein, with a positive charge and a modular structure similar to those of CotG, is common in almost all *Bacillus* species containing a CotH orthologue (Saggese *et al*., 2016). CotG and CotH are functionally linked to each other and their coding genes have a conserved organization with *cotG* entirely contained between the promoter and the coding part of *cotH* (Giglio *et al*., 2011), suggesting that the two proteins may have a similar role in the structure and function of the *Bacillus* spore. Understanding whether the CotH-CotG system responds to the temperature and influences the spore surface structure also in other *Bacillus* species, confirming the role of the positive charge of CotG in the formation of aggregates and clarifying the mechanisms by which *cotG* transcription is controlled by the temperature will all be challenging tasks of future research projects.

Experimental procedures

Bacterial strains and molecular procedures

Bacillus subtilis strains are listed in Table S1 and are all isogenic derivatives of strain PY79 (Youngman *et al*., 1984). Plasmid amplification for nucleotide sequencing, subcloning experiments, and transformation of *Escherichia coli* competent cells were performed with *E*. *coli* strain DH5α. Bacterial strains were transformed by previously described procedures: $CaCl_2$-mediated transformation of *E*. *coli* cells (Sambrook *et al*., 1989), competent cells and two-step transformation of *B*. *subtilis* (Cutting and Vander Horn, 1990). DNA ligation, isolation of plasmids and restriction digestion were performed by using standard methods. Chromosomal DNA extraction

of *B. subtilis* was carried out as described previously (Cutting and Vander Horn, 1990).

B. subtilis *strain construction*

- strain expressing cotG::gusA and cotH::lacZ fusions

A 406 bp DNA fragment containing the *cotG* promoter region and the region coding for 40 amino acids (from the N-terminal end) was PCR amplified using chromosomal DNA of the PY79 strain as a template and priming the reaction with oligonucleotides H2 and G2 (Table S2). The PCR product was cloned in the pTOPO vector (Invitrogen) yielding plasmid pFV200. The *gusA* gene (1812 bp) was excised from the pMLK83 plasmid (Karow and Piggot, 1995) by EcoRI digestion and cloned in pFV200 linearized by EcoRI digestion in frame with *cotG* codons, yielding plasmid pFV201. The gene fusion was then moved into plasmid pER82 (Ricca *et al*., 1992) by subcloning into the BamHI restriction site. The resulting plasmid, pFV202, carried the gene fusion and a kanamycin-resistance gene between two parts of the *amyE* gene of *B. subtilis*. This plasmid was analysed by restriction analysis, linearized by digestion with PstI and used to transform competent cells of the *B. subtilis* strain PY79. Kanamycin-resistant clones were the result of a double-crossover recombination event, resulting in the interruption of the non-essential *amyE* gene on the *B. subtilis* chromosome. All Kanamycin-resistant clones were tested by PCR using chromosomal DNA as a template and oligonucleotides AmyS and AmyA (Table S2) to prime DNA amplification. One positive clone (GC223) was used to extract the chromosomal DNA that was used to transform competent cells of strain GC222 carrying the *cotH::lacZ* fusion integrated at the *cotH* locus (Baccigalupi *et al*., 2004) and yielding strain GC224 (*cotH::lacZ cotG::gusA*).

- strain expressing the cotG::rfp fusion in a mutant lacking CotG and CotH

Chromosomal DNA-mediated transformation of competent cells of the *B. subtilis* strain AZ603 (Δ*cotG* Δ*cotH*::*neo*) (Saggese *et al*., 2014) with chromosomal DNA of *B. subtilis* strain RH296 (*amyE::cotG::rfp*) (Petrillo *et al*., 2020) was used to yield strain RH298 (Δ*cotG* Δ*cotH*::*neo amyE::cotG::rfp*).

- strain expressing the cotG::rfp and cotC::gfp fusions in a mutant lacking CotG and CotH

Chromosomal DNA-mediated transformation of competent cells of the *B. subtilis* strain RH406 (*amyE::cotG::rfp cotC::gfp*) (Petrillo *et al*., 2020) with chromosomal DNA of *B. subtilis* strain AZ603 (*ΔcotG ΔcotH::neo*) (Saggese *et al*., 2014) was used to yield strain AZ720 (*ΔcotG ΔcotH::neo amyE::cotG::rfp cotC::gfp)*.

- strain expressing the cotA::gfp in a mutant lacking CotH

Chromosomal DNA-mediated transformation of competent cells of the *B. subtilis* strain AZ565 (*cotA::gfp*) (Isticato *et al*., 2013) with chromosomal DNA of *B. subtilis* strain AZ607 (Δ*cotG ΔcotH::neo amyE::cotG*) (Saggese *et al*., 2014) was used to yield strain RH240 (Δ*cotG ΔcotH::neo amyE::cotG cotA::gfp)*.

β-Galactosidase and β-glucuronidase assay

The specific β-galactosidase activity was determined using *o*-Nitrophenyl-β-Galactoside as substrate. One millilitre of *cotH::lacZ*-bearing cells was collected, during sporulation, at the times indicated, and assayed as previously described (Ricca *et al*., 1992). The specific β-glucuronidase activity was determined using *p*-Nitrophenyl-β-D-Glucuronide as substrate, as previously reported (Melville *et al*., 1994). One millilitre of *cotG::gusA*-bearing cells was collected, during sporulation, at the times indicated, and assayed as previously described (Melville *et al*., 1994).

Spore coat proteins extraction and Western blot analysis

Sporulation of wild-type and recombinant strains was induced in Difco sporulation medium at 25°C, 37°C or 42°C, with vigorous shaking. During sporulation, at different times, forespores or mature spores were collected as described in Isticato *et al*. (2004) and washed four times with distilled water and purified as described in Nicholson and Setlow (1990). Spore coat proteins were extracted from a suspension of 1×10^9 mature spores or from a suspension of forespores fractions, by treatment at 65°C in SDS-DTT. The extracted proteins were quantified through a Bio-Rad DC protein assay kit (Bio-Rad), then 20 μg of total spore coat proteins were fractionated on 15% polyacrylamide gels and electro-transferred on a nitrocellulose filter (Bio-Rad) for Western blot analysis. Monoclonal antibodies were used at working solution of 1:7.000 for CotG or 1:150 for CotH specific detection. Then, a horseradish peroxidase-conjugated anti-rabbit secondary antibody was used (Santa Cruz). Western blot filters were visualized by the SuperSignal West Pico chemiluminescence (Pierce) method as specified by the manufacturer.

Fluorescence and immunofluorescence microscopy

Fluorescence microscopy analyses were carried out using an Olympus BX51 fluorescence microscope fitted with a 100× objective UPlanF1. FITC (U-MNIB2) and TRITC (U-MWIG2) filters were used to detect the green or red fluorescence signals respectively. Images were captured using an Olympus DP70 digital camera equipped with Olympus U-CA Magnification Changer and

processed with Image Analysis Software (Olympus) for minor adjustments of brightness, contrast and colour balance and for creation of merged images. SmillaEnlarger 0.9.0 software was used to increase images quality. Immunofluorescence assay was performed as described in Manzo *et al*. (2013), with some modifications. One millilitre of sporulating cells was fixed for 1 h at room temperature in 80% methanol, then washed and incubated overnight at 4°C in 100% methanol. Fixed sporangia were permeabilized by incubating samples with a GTE (5% glucose, 0.01 M EDTA pH 8.0, 20 mM Tris–HCl pH 7.5) – 0,2 mg ml^{-1} lysozyme solution and rapidly placed on a coverslip previously treated for 5 min with poly-L-Lysine. The coverslips were air dried, and cells were pretreated with 1% (wt./vol.) dried milk in phosphate-buffered saline (PBS, pH 7.4), prior to 2 h incubation at 4°C with the monoclonal anti-CotC (1:200), anti-CotG (1:500) or anti-PKC (1:500) primary antibodies. After four washes with PBS, the samples were incubated with a 64-fold diluted anti-rabbit secondary antibody, conjugated with Fluorescein isothiocyanate, FITC (BETHYL) for 2 h at room temperature in the dark. After four washes, the coverslips were mounted onto microscope slides, adding one drop of PBS, and analysed by fluorescence microscopy, as described below. Sporangia with only addition of the secondary-FITC conjugated antibody were used as a control of the specificity of this technique.

Acknowledgements

The authors thank G. Cangiano and F. Villanova for their contribution in the construction of the *cotG*::*gusA* fusion and L. Baccigalupi for critical reading of the manuscript. This work was in part supported by the Federico II University of Naples (Ricerca di Dipartimentale to R.I. and E.R.). G.D.G.B. and M.V. were supported by PhD fellowships of the Doctoral programme in Biology of the Federico II University of Naples. C.P. was supported by PhD fellowships of the Doctoral programme in Biotechnology of the Federico II University of Naples. Open Access Funding provided by Universita degli Studi di Napoli Federico II within the CRUI-CARE Agreement. [Correction added on 6 June 2022, after first online publication: CRUI funding statement has been added.]

References

Abhyankar, W.R., Kamphorst, K., Swarge, B.N., van Veen, H., van der Wel, N.N., Brul, S., *et al*. (2016) The influence of sporulation conditions on the spore coat protein composition of *Bacillus subtilis* spores. *Front Microbiol* **7**: 1636.

Baccigalupi, L., Castaldo, G., Cangiano, G., Isticato, R., Marasco, R., De Felice, M., and Ricca, E. (2004) GerE-independent expression of cotH leads to CotC accumulation in the mother cell compartment during *Bacillus subtilis* sporulation. *Microbiology (UK)* **150**: 3441–3449.

Bressuire-Isoard, C., Bornard, I., Henriques, A.O., Carlin, F., and Broussolle, V. (2016) Sporulation temperature reveals a requirement for CotE in the assembly of both the coat and exosporium layers of *Bacillus cereus* spores. *Appl Environ Microbiol* **82**: 232–243.

Christie, G., and Setlow, P. (2020) *Bacillus* spore germination: knowns, unknowns and what we need to learn. *Cell Signal* **74**: 109729.

Cupit, C., Lomstein, B.A., and Kjeldsen, K.U. (2019) Contrasting community composition of endospores and vegetative Firmicutes in a marine sediment suggests both endogenous and exogenous sources of endospore accumulation. *Environ Microbiol Rep* **11**: 352–360.

Cutting, S., and Vander Horn, P.B. (1990) Genetic analysis. In *Molecular Biological Methods for* Bacillus, Harwood, C., and Cutting, S. (eds). Chichester, United Kingdom: John Wiley & Sons, pp. 27–74.

Cutting, S.M. (2011) Bacillus probiotics. *Food Microbiol* **28**: 214–220.

Donadio, G., Lanzilli, M., Sirec, T., Ricca, E., and Isticato, R. (2016) Localization of a red fluorescence protein adsorbed on wild type and mutant spores of *Bacillus subtilis*. *Microb Cell Fact* **15**: 153.

Donovan, W., Zheng, L.B., Sandman, K., and Losick, R. (1987) Genes encoding spore coat polypeptides from *Bacillus subtilis*. *J Mol Biol* **196**: 1–10.

Freitas, C., Plannic, J., Isticato, R., Pelosi, A., Zilhão, R., Serrano, M., *et al*. (2020) A protein phosphorylation module patterns the *Bacillus subtilis* spore outer coat. *Mol Microbiol* **114**: 934–951.

Garcia, D., van der Voort, M., and Abee, T. (2010) Comparative analysis of *Bacillus weihenstephanensis* KBAB4 spores obtained at different temperatures. *Int J Food Microbiol* **140**: 146–153.

Giglio, R., Fani, R., Isticato, R., De Felice, M., Ricca, E., and Baccigalupi, L. (2011) Organization and evolution of the *cotG* and *cotH* genes of *Bacillus subtilis*. *J Bacteriol* **193**: 6664–6673.

Isticato, R., Esposito, G., Zilhão, R., Nolasco, S., Cangiano, G., De Felice, M., *et al*. (2004) Assembly of multiple CotC forms into the *Bacillus subtilis* spore coat. *J Bacteriol* **186**: 1129–1135.

Isticato, R., Lanzilli, M., Petrillo, C., Donadio, G., Baccigalupi, L., and Ricca, E. (2020) *Bacillus subtilis* builds structurally and functionally different spores in response to the temperature of growth. *Environ Microbiol* **22**: 170–182.

Isticato, R., Pelosi, A., Zilhão, R., Baccigalupi, L., Henriques, A.O., De Felice, M., and Ricca, E. (2008) CotC-CotU heterodimerization during assembly of the *Bacillus subtilis* spore coat. *J Bacteriol* **190**: 1267–1275.

Isticato, R., Sirec, T., Giglio, R., Baccigalupi, L., Rusciano, G., Pesce, G., *et al*. (2013) Flexibility of the programme of spore coat formation in *Bacillus subtilis*: bypass of CotE requirement by over-production of CotH. *PLoS One* **8**: e74949.

Karow, M.L., and Piggot, P.J. (1995) Construction of *gusA* transcriptional fusion vector for *Bacillus subtilis* and their utilization for studies of spore formation. *Gene* **163**: 69–74.

Ma, C., Malessa, A., Boersma, A.J., Liu, K., and Herrmann, A. (2020) Supercharged proteins and polypeptides. *Adv Mater* **32**: e1905309.

Manzo, N., Di Luccia, B., Isticato, R., D'Apuzzo, E., De Felice, M., and Ricca, E. (2013) Pigmentation and sporulation are alternative cell fates in *Bacillus pumilus* SF214. *PLoS One* **8**: e62093.

McKenney, P.T., Driks, A., and Eichenberger, P. (2013) The *Bacillus subtilis* endospore: assembly and functions of the multilayered coat. *Nat Rev Microbiol* **11**: 33–44.

Melville, S.B., Labbe, R., and Sonenshein, A.L. (1994) Expression from the *Clostridium perfringens cpe* promoter in *C. perfringens* and *Bacillus subtilis*. *Infect Immun* **62**: 5550–5558.

Naclerio, G., Baccigalupi, L., Zilhao, R., De Felice, M., and Ricca, E. (1996) *Bacillus subtilis* spore coat assembly requires *cotH* gene expression. *J Bacteriol* **178**: 4375–4380.

Nguyen, K.B., Sreelatha, A., Durrant, E.S., Lopez-Garrido, J., Muszewska, A., Dudkiewicz, M., *et al*. (2016) Phosphorylation of spore coat proteins by a family of atypical protein kinases. *Proc Natl Acad Sci U S A* **113**: E3482–E3491.

Nicholson, W.L., and Setlow, P. (1990) Sporulation, germination and outgrowth. In *Molecular Biological Methods for* Bacillus, Harwood, C., and Cutting, S. (eds). Chichester, UK: John Wiley & Sons, pp. 391–450.

Nicolas, P., Mader, U., Dervyn, E., Richat, T., Leduc, A., Pigeonneau, N., *et al*. (2012) Condition-dependent transcriptome reveals high-level regulatory architecture in *Bacillus subtilis*. *Science* **335**: 1103–1106.

Petrillo, C., Castaldi, S., Lanzilli, M., Saggese, A., Donadio, G., Baccigalupi, L., *et al*. (2020) The temperature of growth and sporulation modulates the efficiency of spore-display in *Bacillus subtilis*. *Microb Cell Fact* **19**: 185.

Ricca, E., Cutting, S., and Losick, R. (1992) Characterization of *bofA*, a gene involved in intercompartmental regulation of pro-sigma K processing during sporulation in *Bacillus subtilis*. *J Bacteriol* **174**: 3177–3184.

Sacco, M., Ricca, E., Losick, R., and Cutting, S. (1995) An additional GerE-controlled gene encoding an abundant spore coat protein from *Bacillus subtilis*. *J Bacteriol* **177**: 372–377.

Saggese, A., Isticato, R., Cangiano, G., Ricca, E., and Baccigalupi, L. (2016) CotG-like modular proteins are common among spore-forming bacilli. *J Bacteriol* **198**: 1513–1520.

Saggese, A., Scamardella, V., Sirec, T., Cangiano, G., Isticato, R., Pane, F., *et al*. (2014) Antagonistic role of CotG and CotH on spore germination and coat formation in *Bacillus subtilis*. *PLoS One* **9**: e104900.

Sambrook, J., Fritsch, E.F., and Maniatis, T. (1989) *Molecular Cloning: A Laboratory Manual*, 2nd ed. Cold Spring Harbor, NY: Cold Spring Harbor Laboratory Press.

Timmusk, S., Paalme, V., Pavlicek, T., Bergquist, J., Vangala, A., Danilas, T., and Nevo, E. (2011) Bacterial distribution in the rhizosphere of wild barley under contrasting microclimates. *PLoS One* **6**: e17968.

Youngman, P., Perkins, J.B., and Losick, R. (1984) A novel method for the rapid cloning in *Escherichia coli* of *Bacillus subtilis* chromosomal DNA adjacent to Tn917 insertions. *Mol Gen Genet* **195**: 424–433.

Supporting Information

Additional Supporting Information may be found in the online version of this article at the publisher's web-site:

Appendix S1: Supplementary Information.